Design Optimization of SIMO Receivers with Compact Uniform Linear Arrays and Limited Precision A/D Conversion

Qing Bai and Josef A. Nossek
Institute for Circuit Theory and Signal Processing
Technische Universität München, Munich, Germany
Email: bai@tum.de

***Abstract*—Antenna arrays can be made *compact* when the spacing between adjacent antennas is reduced to less than half of the wavelength. This facilitates the deployment of multiple antennas to communication devices that are limited in their physical dimensions, yet introduces significant spatial correlation between the channels as well as antenna mutual coupling. With careful design of a matching network at the receiver front-end, the antennas can be decoupled and superior performance can be achieved as compared to half-wavelength arrays. In this work, we investigate the design optimization of a multi-antenna receiver with a compact uniform linear array, where we try to find the optimal antenna spacing and the number of antennas that lead to the maximal channel capacity and energy efficiency of the system. Moreover, we take into account the impact of A/D conversion with limited precision, which results in a trade-off between quantization error and power consumption. Simulation results accentuate the advantage of using small compact antenna arrays and low bit resolutions for the A/D converters.**

I. Introduction

Multi-antenna communication systems promise significant improvements in the achievable data rate and reliability over single-antenna systems [1][2]. In addition to the higher hardware complexity and more energy consumption, the space required to deploy the multiple antennas impose another limitation on multi-antenna systems, which is even more critical to portable devices and wireless sensors. It has been common practice to use half of the wavelength as the spacing between adjacent antenna elements for linear antenna arrays, which effectively limits the detrimental impact of *spatial correlation* [3][4]. When the antenna elements are moved closer to a spacing below or well below half of the wavelength, pronounced spatial correlation between the channels as well as *antenna mutual coupling* are introduced [5][6]. Contrary to some previous belief, antenna mutual coupling can be beneficial given that appropriate impedance matching is employed. In [7], the authors developed a linear multiport model for multi-antenna systems which is in consistency with the underlying physics. Based on this model, an impedance matching network which decouples the receive antennas in a compact array of isotrops is derived analytically. The paper further presents a compact signal model that results from the employment of the matching networks, which provides the desired level of abstraction for subsequent information theoretic studies. Exploiting this theoretical framework, we are able to perform numerical optimizations on the array configuration including the antenna spacing and the number of antennas, with the goal of maximizing the ergodic channel capacity and/or the energy efficiency of the system. Part of this investigation has been presented in our previous work [8].

The major new contribution of this paper is to include the analog-to-digital converter (ADC) into the design optimization of the multi-antenna receiver. The important role that the A/D conversion plays in a communication system has called more and more research attention due to the design goals of achieving higher and higher data rate, and/or of reducing the complexity and power consumption of the system. It has been reported [9] that the ADC consumes a significant amount of power when operating at high sampling rate and resolution, hence becoming a bottleneck in the system performance. Based on the results of capacity degradation with low-precision A/D conversion [10][11] and the power consumption model of the ADC [12], we are able to exploit and quantify the trade-off between quantization loss and power dissipation, which is governed by the bit resolution that is chosen for the ADC. To this end, a joint optimization of the compact antenna array and the subsequent A/D conversion operation can be formulated, which aims at maximizing the energy efficiency of the system defined by the number of successfully conveyed information bits per consumed Joule of energy at the receiver. A number of questions may arise upon this conception such as, whether and to which extent will the optimal antenna spacing be influenced by the limited precision A/D conversion, can the compact array and low-resolution ADC design be applied at the same time. In this work we seek the answers to those questions, which are certainly of interest to real system deployment and operation.

The rest of the paper is organized as follows: in Section II we introduce the SIMO system model starting from the circuit theoretic linear multiport model, coming then to the information theoretic description of the system which facilitates the study of the impacts of low-precision A/D conversion, and finally giving a power consumption model for the receiver. The energy efficiency of the system is defined in Section III, and its maximization with respect to the array configuration and the ADC resolution is formulated and analyzed. Numerical simulation results are presented in Section IV, where a number of interesting insight on the design and operation of the system are given. Lastly, the paper is summarized and concluded in Section V.

Notations: we use small boldfaced letters to represent vectors, and big boldfaced letters to represent matrices throughout

ISBN 978-3-8007-3662-1

the paper. The symbol $\mathbf{1}_M$ denotes the identity matrix of dimension $M \times M$. For an arbitrary matrix $\boldsymbol{A}$, $\boldsymbol{A}^{\mathrm{T}}$ and $\boldsymbol{A}^{\mathrm{H}}$ stand for the transpose and the Hermitian of $\boldsymbol{A}$. For a square matrix $\boldsymbol{A}$, $\mathrm{diag}(\boldsymbol{A})$ denotes the diagonal matrix with the same diagonal elements as $\boldsymbol{A}$.

II. System Model

We consider a single-input multiple-output (SIMO) system which employs a uniform linear array of closely spaced receive antennas. In the first part of this section, we establish the input-output relationship of the system before quantization by using circuit theory [7], which captures the essential characteristics and impacts of the compact antenna array, and then connect the involved physical quantities with the abstractions that are commonly used in information theory. In the second part, we introduce the modeling of the A/D conversion based on the Bussgang theorem [13][11], which enables us to compute a lower bound on the ergodic capacity of the quantized channel as a function of the bit resolution employed by the A/D converters. Lastly, we discuss the power consumption of the receiver as dependent on the key design parameters.

A. Multiport model and circuit analysis

The physical modeling of the system before quantization of the received signal, as demonstrated with Figure 1, is based on the circuit theoretic concept of linear multiports [7], a tool of which has been used to bridge the gap between the physical and information theoretic descriptions of a multi-antenna communication system. Here we briefly review the modeling process presented in the aforementioned paper, with the necessary definitions, derivations, and conclusions.

1) Transmit side: Shown in the very left of Figure 1, the generation of the transmit signal is modeled by a voltage source whose complex voltage envelope is denoted with $v_{\mathrm{G}} \in \mathbb{C} \cdot \mathrm{V}$. In order to deliver the maximum power to the transmit antenna, the subsequent impedance matching network $\boldsymbol{Z}_{\mathrm{MT}} \in \mathbb{C}^{2\times 2} \cdot \Omega$ is employed which should guarantee that the impedance seen at its input is equal to the resistance R that is connected in serial with the voltage source. With such *power matching* strategy, we have

$$v_{\mathrm{T}} = \frac{1}{2} v_{\mathrm{G}}, \quad P_{\mathrm{tx}} = \mathrm{E}\left[\mathrm{Re}\{v_{\mathrm{T}}^{*} i_{\mathrm{T}}\}\right] = \frac{\mathrm{E}\left[|v_{\mathrm{G}}|^2\right]}{4R}, \tag{1}$$

where P_{tx} stands for the power that flows into the matching network, which is equivalently the power delivered to the transmit antenna given the assumption of a lossless matching network.

2) Antenna mutual coupling: The mutual coupling between the transmit and receive antennas is captured by the impedance matrix $\boldsymbol{Z}_{\mathrm{A}} \in \mathbb{C}^{(M+1)\times(M+1)} \cdot \Omega$, which describes the linear $(M+1)$ port according to

$$\begin{bmatrix} v_{\mathrm{A}} \\ \boldsymbol{v}_{\mathrm{B}} \end{bmatrix} = \begin{bmatrix} Z_{\mathrm{AT}} & \boldsymbol{Z}_{\mathrm{ATR}} \\ \boldsymbol{Z}_{\mathrm{ART}} & \boldsymbol{Z}_{\mathrm{AR}} \end{bmatrix} \begin{bmatrix} i_{\mathrm{A}} \\ \boldsymbol{i}_{\mathrm{B}} \end{bmatrix} \tag{2}$$

$$\approx \begin{bmatrix} Z_{\mathrm{AT}} & \mathbf{0}^{\mathrm{T}} \\ \boldsymbol{Z}_{\mathrm{ART}} & \boldsymbol{Z}_{\mathrm{AR}} \end{bmatrix} \begin{bmatrix} i_{\mathrm{A}} \\ \boldsymbol{i}_{\mathrm{B}} \end{bmatrix}. \tag{3}$$

Notice that in (2), the matrix $\boldsymbol{Z}_{\mathrm{A}}$ is partitioned into the transmit impedance Z_{AT}, the receive impedance matrix $\boldsymbol{Z}_{\mathrm{AR}}$, and the transimpedance vectors $\boldsymbol{Z}_{\mathrm{ART}}$ and $\boldsymbol{Z}_{\mathrm{ATR}}$. By arguing that the signal is greatly attenuated when propagating from the transmitter to the receiver, we make the *unilateral approximation* in (3) since $||\boldsymbol{Z}_{\mathrm{ATR}}||_{\mathrm{F}} \ll ||Z_{\mathrm{AT}}||_{\mathrm{F}}$. The direct consequence that $v_{\mathrm{A}} = Z_{\mathrm{AT}} i_{\mathrm{A}}$ implies the independence of the transmitter from the receiver, thus significantly simplifies our analysis.

3) Receive side: We assume that the antennas in our system are *isotropic* radiators for simplicity of the analytical analysis. Although they do not exist in practice, there are real kinds of antennas such as short dipoles and half-wavelength dipoles that come close in performance to the isotropic radiators in our context. The background radiation picked up by the receive antennas is modeled by the M voltage sources with complex voltage envelopes $\tilde{v}_{\mathrm{N},1}, \ldots, \tilde{v}_{\mathrm{N},M}$, which form the vector $\tilde{\boldsymbol{v}}_{\mathrm{N}} \in \mathbb{C}^{M\times 1} \cdot \mathrm{V}$. We term this noise as the *extrinsic noise* so as to distinguish from the noise caused by the circuit components of the receiver. Assuming isotropic extrinsic noise, we have the covariance matrix of $\tilde{\boldsymbol{v}}_{\mathrm{N}}$ given as

$$\mathrm{E}\left[\tilde{\boldsymbol{v}}_{\mathrm{N}} \tilde{\boldsymbol{v}}_{\mathrm{N}}^{\mathrm{H}}\right] = \tilde{\beta} R_{\mathrm{r}}^2 \left(\boldsymbol{C} + \kappa\, \mathbf{1}_M\right),$$

where R_{r} and R_{d} are the radiation resistance and the dissipation resistance of the antennas, respectively. The scalars $\tilde{\beta} \in \mathbb{R} \cdot \mathrm{A}$ and $\kappa \in \mathbb{R}$ are defined as

$$\tilde{\beta} = \frac{4\mathrm{k} T_{\mathrm{A}} B}{R_{\mathrm{r}}}, \quad \kappa = \frac{R_{\mathrm{d}}}{R_{\mathrm{r}}},$$

where k denotes the Boltzmann constant, T_{A} denotes the noise temperature of the antennas, and B is the signal bandwidth. Let the receive antenna elements be enumerated sequentially with integer numbers $0, 1, \ldots, M-1$. Based on the isotropicity assumption, the matrix $\boldsymbol{C}$ can be derived as

$$\boldsymbol{C} = \begin{bmatrix} 1 & j_0(d_{01}) & j_0(d_{02}) & j_0(d_{03}) & \cdots \\ j_0(d_{10}) & 1 & j_0(d_{12}) & j_0(d_{13}) & \ddots \\ \vdots & \ddots & \ddots & \ddots & \ddots \end{bmatrix}$$

$$\text{with} \quad j_0(x) = \frac{\sin kx}{kx},\ k = \frac{2\pi}{\lambda},$$

where λ is the signal wavelength and d_{ij} is the distance between antenna i and antenna j, $i, j = 0, 1, \ldots, M-1$. Note that $\boldsymbol{C}$ is a real-valued matrix with diagonal elements of unity. For the ULA, the distance between adjacent antennas is identical. Denoting that uniform spacing with d, we simply have $d_{ij} = |i-j|d$, which renders the matrix $\boldsymbol{C}$ Toeplitz and positive definite. When d is multiples of half wavelength, $\boldsymbol{C}$ reduces to the identity matrix.

At the receive side, an impedance matching network is employed to decouple the antennas and improve the receive signal-to-noise ratio (SNR). Let the impedance matrix be $\boldsymbol{Z}_{\mathrm{MR}} \in \mathbb{C}^{2M\times 2M} \cdot \Omega$ and assume likewise that the matching network is lossless. The desired matching strategy, the so-called *noise matching*, further requires careful modeling of the *intrinsic noise* caused by the functional components at the receiver front-end, among which the low-noise amplifiers (LNA) have the most important contribution. For each receive branch, we model the LNA and all subsequent circuitry as a two port, and use one voltage source and one current source at the input of the port in order to fully describe the properties of the intrinsic noise. Let the complex voltage envelopes and the complex current envelopes at all branches be M-dimensional

ISBN 978-3-8007-3662-1

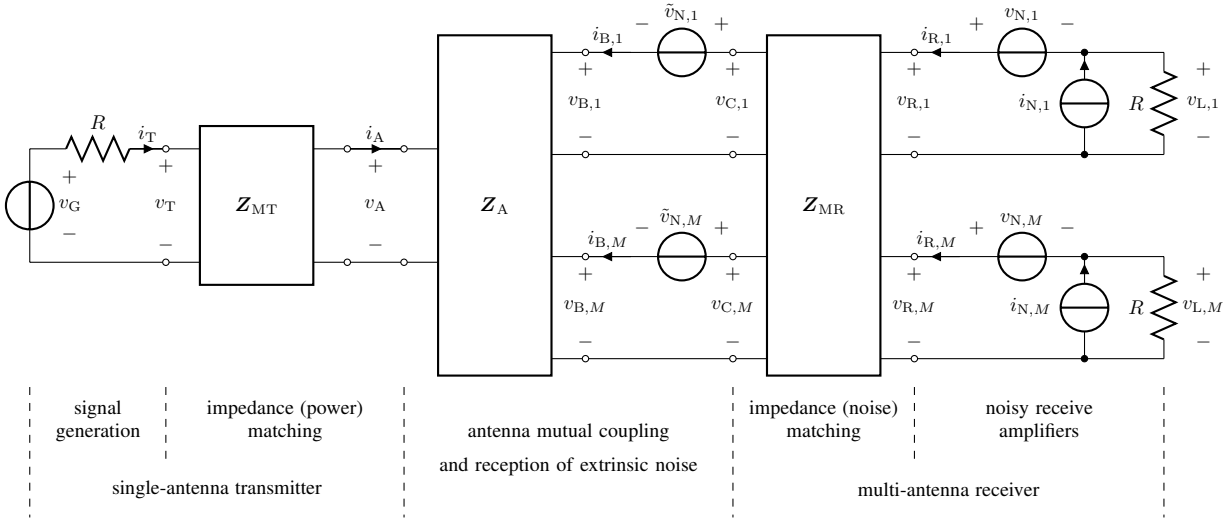

Figure 1. Linear multiport model of a SIMO system

vectors $\boldsymbol{v}_{\mathrm{N}}$ and $\boldsymbol{i}_{\mathrm{N}}$, respectively, and the input impedance of each LNA be equal to R. We define the following covariance matrices for the intrinsic noise

$$\begin{aligned}\mathrm{E}\left[\boldsymbol{i}_{\mathrm{N}}\boldsymbol{i}_{\mathrm{N}}^{\mathrm{H}}\right] &= \beta\,\mathbf{1}_M,\\ \mathrm{E}\left[\boldsymbol{v}_{\mathrm{N}}\boldsymbol{v}_{\mathrm{N}}^{\mathrm{H}}\right] &= \beta R_{\mathrm{N}}^2\,\mathbf{1}_M,\\ \mathrm{E}\left[\boldsymbol{v}_{\mathrm{N}}\boldsymbol{i}_{\mathrm{N}}^{\mathrm{H}}\right] &= \rho\beta R_{\mathrm{N}}\,\mathbf{1}_M,\end{aligned}$$

with the *noise resistance* R_{N} and the *noise correlation coefficient* $\rho \in \mathbb{C}$ given by

$$R_{\mathrm{N}} = \sqrt{\frac{\mathrm{E}\left[|v_{\mathrm{N},j}|^2\right]}{\mathrm{E}\left[|i_{\mathrm{N},j}|^2\right]}}, \quad \rho = \frac{\mathrm{E}\left[v_{\mathrm{N},j}i_{\mathrm{N},j}^*\right]}{\mathrm{E}\left[|v_{\mathrm{N},j}|^2\right]\mathrm{E}\left[|i_{\mathrm{N},j}|^2\right]},$$

$\forall j \in \{0,\ldots,M-1\}$. The above definitions are based on the assumptions that the circuitry in each receive branch possesses identical statistical properties and that the noise sources are independent from each other. For $\rho \neq 0$, the noise voltage envelope and the noise current envelope originated from the same amplifier are correlated.

4) Input-output relation: The complex voltage envelopes $v_{\mathrm{L},1},\ldots,v_{\mathrm{L},M}$ that appear at the loads form the vector $\boldsymbol{v}_{\mathrm{L}} \in \mathbb{C}^{M\times 1}\cdot\mathrm{V}$, which, due to the linearity of the circuit, can be expressed as a linear function of the source voltage envelope v_{G} with an additive noise term $\boldsymbol{n} \in \mathbb{C}^{M\times 1}\cdot\sqrt{\mathrm{W}}$ as

$$\boldsymbol{v}_{\mathrm{L}} = \boldsymbol{d}\,v_{\mathrm{G}} + \sqrt{R}\,\boldsymbol{n}, \tag{4}$$

where the scaling of $\boldsymbol{n}$ by $\sqrt{R}$ ensures that $||\boldsymbol{n}||^2$ has the physical dimension of power. In the meanwhile, excluding signal generation, the addition of extrinsic as well as intrinsic noise, we may write for the multiport defined by the impedance matching network of the transmitter, the transmit and receive antennas, and the impedance matching network of the receiver in the noise-free case the following relation

$$\left.\begin{bmatrix} v_{\mathrm{T}} \\ \boldsymbol{v}_{\mathrm{R}}\end{bmatrix}\right|_{\tilde{\boldsymbol{v}}_{\mathrm{N}}=\mathbf{0}} = \begin{bmatrix} Z_{\mathrm{T}} & \mathbf{0}^{\mathrm{T}} \\ \boldsymbol{Z}_{\mathrm{RT}} & \boldsymbol{Z}_{\mathrm{R}}\end{bmatrix}\begin{bmatrix} i_{\mathrm{T}} \\ \boldsymbol{i}_{\mathrm{R}}\end{bmatrix}.$$

With power matching at the transmitter and noise matching at the receiver, we should have

$$\begin{aligned}&Z_{\mathrm{T}} = R,\\ &\boldsymbol{Z}_{\mathrm{R}} = Z_{\mathrm{opt}}\,\mathbf{1}_M = R_{\mathrm{N}}\Big(\sqrt{1-\mathrm{Im}^2\{\rho\}} + \mathrm{j}\,\mathrm{Im}\{\rho\}\Big)\,\mathbf{1}_M\end{aligned}$$

with optimized $\boldsymbol{Z}_{\mathrm{MT}}$ and $\boldsymbol{Z}_{\mathrm{MR}}$, where Z_{opt} is the transformed antenna impedance that leads to the minimum noise figure $\mathrm{NF}_{\min}$ of each branch of the receiver front-end. It can then be derived using circuit analysis that

$$\begin{aligned}\boldsymbol{d} &= \frac{\sqrt{R\cdot\mathrm{Re}\{Z_{\mathrm{opt}}\}}}{2(R+Z_{\mathrm{opt}})}\,\mathrm{Re}\{\boldsymbol{Z}_{\mathrm{AR}}\}^{-\frac{1}{2}}\boldsymbol{Z}_{\mathrm{ART}}\,\mathrm{Re}\{Z_{\mathrm{AT}}\}^{-\frac{1}{2}},\\ \boldsymbol{n} &= \frac{\sqrt{R}}{R+Z_{\mathrm{opt}}}\Big(Z_{\mathrm{opt}}\,\boldsymbol{i}_{\mathrm{N}} - \boldsymbol{v}_{\mathrm{N}} + \boldsymbol{F}_{\mathrm{R}}\tilde{\boldsymbol{v}}_{\mathrm{N}}\Big),\end{aligned}$$

where $\boldsymbol{F}_{\mathrm{R}} = \mathrm{j}\sqrt{\mathrm{Re}\{Z_{\mathrm{opt}}\}}\,\mathrm{Re}\{\boldsymbol{Z}_{\mathrm{AR}}\}^{-\frac{1}{2}}$. Interestingly, it can be noticed that the imaginary parts of $\boldsymbol{Z}_{\mathrm{AR}}$ and Z_{AT} do not play any role here; and for lossy isotropic radiators, we are able to find their real parts in closed form as

$$\begin{aligned}\mathrm{Re}\{Z_{\mathrm{AT}}\} &= R_{\mathrm{r}} + R_{\mathrm{d}} = R_{\mathrm{r}}(1+\kappa),\\ \mathrm{Re}\{\boldsymbol{Z}_{\mathrm{AR}}\} &= R_{\mathrm{r}}\,\boldsymbol{C} + R_{\mathrm{d}}\,\mathbf{1}_M = R_{\mathrm{r}}(\boldsymbol{C} + \kappa\,\mathbf{1}_M),\end{aligned}$$

which enables the calculation of the covariance matrix of the noise vector $\boldsymbol{n}$ as

$$\boldsymbol{R}_{nn} = \mathrm{E}\left[\boldsymbol{n}\boldsymbol{n}^{\mathrm{H}}\right] = \frac{RR_{\mathrm{r}}\,\tilde{\beta}\,\mathrm{NF}_{\min}\,\mathrm{Re}\{Z_{\mathrm{opt}}\}}{|R+Z_{\mathrm{opt}}|^2}\cdot\mathbf{1}_M. \tag{5}$$

On the other hand, the transimpedance vector $\boldsymbol{Z}_{\mathrm{ART}}$ can be expressed as a weighted sum of receive array steering vectors corresponding to each arriving path, where the weighting factors have the physical dimension of resistance and are inverse proportional to the distances that the paths have traveled. For a correlated Rayleigh fading channel, we can write $\boldsymbol{Z}_{\mathrm{ART}}$ in a compact manner as

$$\frac{\boldsymbol{Z}_{\mathrm{ART}}}{R_{\mathrm{r}}\sqrt{1+\kappa}} = \sqrt{\alpha}\,\boldsymbol{R}^{\frac{1}{2}}\boldsymbol{g}, \tag{6}$$

ISBN 978-3-8007-3662-1

where $\boldsymbol{R} \in \mathbb{C}^{M\times M}$ is the so-called receive correlation matrix with unit diagonal elements, $\alpha \in \mathbb{R}^+$ resembles the average gain of the propagation channel, and $\boldsymbol{g} \in \mathbb{C}^{M\times 1}$ contains i. i. d. standard complex Gaussian distributed elements. The normalization in (6) renders the right-hand side dimensionless and the vector $\boldsymbol{d}$ a concise form.

5) Spatial correlation model: Spatial correlation in the received signals of a multi-antenna system is introduced by sparse scattering in the propagation environment, and can be more pronounced when the separation of the receive antennas is not large enough. Taking into account that the scatterers and reflectors on the way of propagation posses both different azimuths and elevations, we employ in this work a 3D spatial correlation model which is illustrated in Figure 2.

The reference antenna, namely antenna 0, is located at the origin of the 3D coordinate frame. The receive signal is assumed to arrive with a group of signal paths where the central arriving direction is in parallel with the z-axis. Let the *angle of arrival* (AoA) be the angle between the ULA-axis and the direction from which the wavefront is impinging on the array. Consequently, the *end-fire* direction refers to the AoA of 0 degree, whereas the *front-fire* direction refers to the AoA of 90 degrees. We further restrict the ULA-axis to lie in the y-z plane and denote the mean AoA with θ_0. Let the angle deviation of a signal path from the z-axis be θ, and assume it is continuously distributed on $[\,0, \Delta\theta\,]$. On the other hand, the angle between the x-axis and the projection of the signal path to the x-y plane, denoted with ϕ, is continuously distributed on $[\,0, 2\pi\,]$. In Figure 2, we illustrate one signal path with the straight red line. The corresponding AoA, denoted with φ, can be obtained via

$$\cos\varphi = \sin\theta\sin\phi\sin\theta_0 + \cos\theta\cos\theta_0$$

using geometry, from which we can directly compute the array steering vector

$$\boldsymbol{a}(\theta,\phi) = \left[\begin{array}{cccc} 1 & \mathrm{e}^{-\mathrm{j}kd\cos\varphi} & \cdots & \mathrm{e}^{-\mathrm{j}(M-1)kd\cos\varphi} \end{array}\right]^{\mathrm{T}}.$$

Assuming the signals impinge with uniform power density (constant power per area), the spatial correlation feature of the antenna array is captured by the matrix

$$\boldsymbol{R} = \xi \int_{\phi=0}^{2\pi}\int_{\theta=0}^{\Delta\theta} \sin\theta\cdot\boldsymbol{a}(\theta,\phi)\boldsymbol{a}^{\mathrm{H}}(\theta,\phi)\,\mathrm{d}\theta\mathrm{d}\phi,$$

where the constant scalar $\xi \in \mathbb{R}^+$ normalizes the diagonal elements of the matrix to unity. Note that the positive semi-definite matrix $\boldsymbol{R}$ depends on the antenna spacing d and the mean AoA θ_0 via the array steering vector $\boldsymbol{a}$, and is also dependent on the angle spread of the multipath components indicated by $2\Delta\theta$. The matrix $\boldsymbol{R}^{\frac{1}{2}}$ as in (6) is a matrix square root of $\boldsymbol{R}$, that is, it satisfies $\boldsymbol{R} = \boldsymbol{R}^{\frac{1}{2}}\boldsymbol{R}^{\frac{1}{2},\mathrm{H}}$.

B. Information theoretic description

Our task now is to make clear the connection between the circuit theoretic description of the SIMO system (4) and the following description which is commonly found in the information theory literature:

$$\boldsymbol{y} = \boldsymbol{h}\,x + \boldsymbol{\theta}, \tag{7}$$

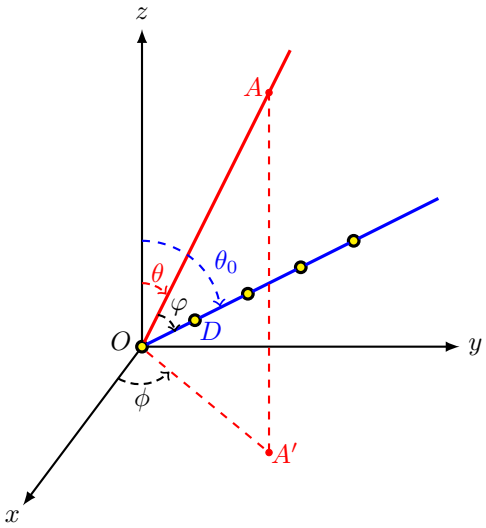

Figure 2. Obtaining a 3D spatial correlation model for a ULA of isotrops

where $x \in \mathbb{C}$, $\boldsymbol{h} \in \mathbb{C}^{M\times 1}$, and $\boldsymbol{y} \in \mathbb{C}^{M\times 1}$ are termed as the channel input, the vector of channel coefficients, and the channel output, respectively. The additive noise is usually assumed white and zero-mean complex circularly symmetric Gaussian distributed. The covariance matrix of $\boldsymbol{\theta}$ is given as

$$\mathrm{E}\left[\boldsymbol{\theta}\boldsymbol{\theta}^{\mathrm{H}}\right] = \sigma^2\,\mathbf{1}_M \quad \text{with} \quad \sigma^2 = 4\mathrm{k}T_{\mathrm{A}}B\,\mathrm{NF}_{\min}.$$

The transmit power in this context is conventionally defined as $P_{\mathrm{tx}} = \mathrm{E}\left[|x|^2\right]$. Comparing with (1) and (5), we easily come to the mapping strategy

$$x = \frac{v_{\mathrm{G}}}{2\sqrt{R}}, \quad \boldsymbol{\theta} = \sqrt{\sigma^2}\,\boldsymbol{R}_{nn}^{-\frac{1}{2}}\boldsymbol{n}. \tag{8}$$

Plugging v_{G} as a function of x and $\boldsymbol{n}$ as a function of $\boldsymbol{\theta}$ back into (4), we further obtain, based on the equivalence of (4) and (7), the following relations:

$$\begin{aligned}\boldsymbol{y} &= \sqrt{\frac{\sigma^2}{R}}\,\boldsymbol{R}_{nn}^{-\frac{1}{2}}\boldsymbol{v}_{\mathrm{L}},\\ \boldsymbol{h} &= 2\sqrt{\sigma^2}\,\boldsymbol{R}_{nn}^{-\frac{1}{2}}\boldsymbol{d}\\ &= \mathrm{e}^{\mathrm{j}\varphi}\,\mathrm{Re}\{\boldsymbol{Z}_{\mathrm{AR}}\}^{-\frac{1}{2}}\boldsymbol{Z}_{\mathrm{ART}}\,\mathrm{Re}\{Z_{\mathrm{AT}}\}^{-\frac{1}{2}}\\ &= \mathrm{e}^{\mathrm{j}\varphi}\,\sqrt{\alpha}\,(\boldsymbol{C}+\kappa\,\mathbf{1}_M)^{-\frac{1}{2}}\boldsymbol{R}^{\frac{1}{2}}\boldsymbol{g},\end{aligned}$$

where $\mathrm{e}^{\mathrm{j}\varphi} = |R+Z_{\mathrm{opt}}|/(R+Z_{\mathrm{opt}})$ contributes merely a phase shift to all channel coefficients. Consequently, for a SIMO system with a compact receive antenna array of lossy and mutually coupled isotrops, we are able to write the input-output relationship as

$$\boldsymbol{y} = \mathrm{e}^{\mathrm{j}\varphi}\,\sqrt{\alpha}\,(\boldsymbol{C}+\kappa\,\mathbf{1}_M)^{-\frac{1}{2}}\boldsymbol{R}^{\frac{1}{2}}\boldsymbol{g}\,x + \boldsymbol{\theta}, \tag{9}$$

given that power matching is employed at the transmitter, noise matching is employed at the receiver, and isotropic background radiation is received. The key impacts of the compact antenna array are fully and conveniently reflected in (9), which lays the basis of the subsequent modeling and performance optimizations.

ISBN 978-3-8007-3662-1

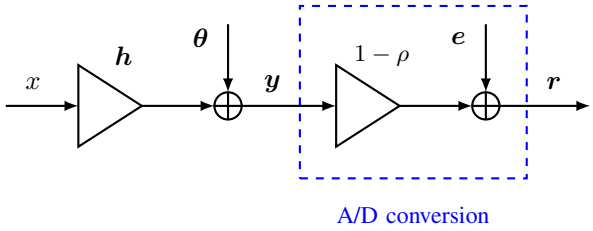

Figure 3. SIMO receiver with linearized quantization operation

C. A/D conversion with limited precision

The received signal $\boldsymbol{y} \in \mathbb{C}^{M\times 1}$ is continuous both in time and magnitude, and needs to be converted to digital format before further processing. There are two A/D converters associated with each antenna to accomplish this, one for the real part of the signal, and the other for the imaginary part. We assume that the $2M$ A/D converters at the receiver are identical and they employ the same *bit resolution* for quantization, that is, the same number of bits to represent one sample. We denote the bit resolution with b and assume that $b \in \{1, \ldots, b_{\max}\}$, where $b_{\max}$ is the highest possible bit resolution allowed by the system. By using the Bussgang theorem [13], we are able to decompose the non-linear quantization operation as a linear transformation plus an additive noise which is uncorrelated with the input [11]. To this end, defining $\boldsymbol{A} = (\boldsymbol{C} + \kappa\, \mathbf{1}_M)^{-\frac{1}{2}} \boldsymbol{R}^{\frac{1}{2}}$, we have the quantized receive signal $\boldsymbol{r} \in \mathbb{C}^{M\times 1}$ expressed as

$$\begin{aligned} \boldsymbol{r} &= (1-\rho)\boldsymbol{y} + \boldsymbol{e} \\ &= (1-\rho)\mathrm{e}^{\mathrm{j}\varphi}\sqrt{\alpha}\,\boldsymbol{A}\boldsymbol{g}\,x + (1-\rho)\boldsymbol{\theta} + \boldsymbol{e} \\ &\triangleq \boldsymbol{h}'x + \boldsymbol{\theta}', \end{aligned} \tag{10}$$

where $\boldsymbol{h}', \boldsymbol{\theta}' \in \mathbb{C}^{M\times 1}$ as defined indicate the *effective channel vector* and the *effective noise vector*, respectively. The real-valued scalar ρ stands for the distortion factor of the quantization, which is dependent on the bit resolution b and attains the values given in Table I [14] for distortion-minimizing scalar quantizers and Gaussian input signals. The quantization error $\boldsymbol{e}$ and the effective noise $\boldsymbol{\theta}'$ have been shown [15] to possess the covariance matrices

$$\begin{aligned} \boldsymbol{R}_{ee} &= \rho(1-\rho)\,\mathrm{diag}(\boldsymbol{R}_{yy}) \\ &= \rho(1-\rho)\sigma^2\,\mathrm{diag}\left(\gamma\,\boldsymbol{A}\boldsymbol{g}\boldsymbol{g}^{\mathrm{H}}\boldsymbol{A}^{\mathrm{H}} + \mathbf{1}_M\right), \\ \boldsymbol{R}_{\theta'\theta'} &= (1-\rho)^2\boldsymbol{R}_{\theta\theta} + \boldsymbol{R}_{ee} \\ &= (1-\rho)^2\sigma^2\big(\mathbf{1}_M + \tfrac{\rho}{1-\rho}\,\mathrm{diag}\left(\gamma\,\boldsymbol{A}\boldsymbol{g}\boldsymbol{g}^{\mathrm{H}}\boldsymbol{A}^{\mathrm{H}} + \mathbf{1}_M\right)\big), \end{aligned}$$

where perfect channel state information (CSI) is assumed and $\gamma = \alpha P_{\mathrm{tx}}/\sigma^2$ denotes the average receive SNR.

Table I. DISTORTION FACTOR ρ FOR DIFFERENT BIT RESOLUTIONS b

b	1	2	3	4
ρ	0.3634	0.1175	0.03454	0.009497
b	5	6	7	8
ρ	0.002499	0.0006642	0.0001660	0.00004151

The mutual information between the channel input x and the quantized output $\boldsymbol{r}$ achieves the minimum when the effective noise is Gaussian distributed. In that case, we obtain a lower bound on the ergodic capacity of the quantized SIMO channel in bit/sec/Hz as

$$\begin{aligned} C_{\mathrm{L}} &= \mathrm{E}_{\boldsymbol{g}}\left[\log_2\left(1 + P_{\mathrm{tx}}\boldsymbol{h}'^{\mathrm{H}}\boldsymbol{R}^{-1}_{\theta'\theta'}\boldsymbol{h}'\right)\right] \\ &= \mathrm{E}_{\boldsymbol{g}}\Big[\log_2\big(1 + \gamma\,\boldsymbol{g}^{\mathrm{H}}\boldsymbol{A}^{\mathrm{H}}\big(\mathbf{1}_M \\ &\qquad + \tfrac{\rho}{1-\rho}\,\mathrm{diag}\left(\gamma\,\boldsymbol{A}\boldsymbol{g}\boldsymbol{g}^{\mathrm{H}}\boldsymbol{A}^{\mathrm{H}} + \mathbf{1}_M\right)\big)^{-1}\boldsymbol{A}\boldsymbol{g}\big)\Big]. \end{aligned} \tag{11}$$

This capacity lower bound has been proven tight in the low SNR regime [11], and we use it here for the design optimization due to the convenience and theoretical performance limit it provides. Note that C_{L} is a function of the antenna spacing d and likewise a function of the number of receive antennas M, where the dependency on the array configuration is encapsulated by the matrix $\boldsymbol{A}$.

D. Power consumption of the receiver

For wireless communications over short distances, which is now more common due to the wide deployment of wireless local area networks as well as femto- and picocells, power consumption incurred by the circuits of the transceivers becomes non-negligible and even dominant in the total power consumption of the system [16][17]. We employ here a concise power consumption model for the multi-antenna receiver which mainly addresses the impact of the number of antennas and the bit resolution adopted by the ADC. The main contributors to the power consumption of each RF chain of the receiver include the LNA, the ADC, the mixer, and the receive filter. Their contribution to the total power consumption of the system grows linearly with the number of RF chains, which, in our system design, is equal to the number of antennas. Part of the baseband processing power might also depend on the number of antennas, such as those used for channel estimation [18]. Power consumption of other circuit components and processing tasks is modeled as a constant c_0. Addressing the trade-off between power and quantization error, we give the power dissipation of the ADC as a function of the employed bit resolution $b > 0$:

$$P_{\mathrm{ADC}} = c_{\mathrm{ADC}}\,\beta \cdot 2^b,$$

where c_{ADC} is a constant parameter specific to the ADC design [12]. The expression indicates that the power dissipation of the ADC is proportional to the signal bandwidth and the noise power spectral density, and grows exponentially with the employed bit resolution. The remaining power consumption of the system that is to be scaled with M is represented by the constant c_2. Consequently, we model the total power consumption of the receiver in Watt as

$$P = M\big(2P_{\mathrm{ADC}} + c_2\big) + c_0 = M\big(c_1\,2^b + c_2\big) + c_0, \tag{12}$$

where $c_1 = 2c_{\mathrm{ADC}}\,\beta$. For the numerical simulations, we take the values $c_0 = 0.2$ Watt, $c_1 \in \{0.01, 0.005\}$ Watt, $c_2 = 0.05$ Watt, $b_{\max} = 8$, and $B = 1$ MHz with reference to [17].

III. ENERGY EFFICIENCY MAXIMIZATION

The *energy efficiency* (EE) of the multi-antenna receiver under consideration can be measured by the bit / Joule metric, *i.e.*, the number of successfully received information bits divided by the correspondingly consumed energy. In our case, this metric is approximated with the ratio between the lower bound on the ergodic capacity C_{L} times the signal bandwidth

ISBN 978-3-8007-3662-1

B and the power consumption of the receiver P for better tractability:

$$\text{EE}: \quad \eta = \frac{B\, C_{\text{L}}(d, b, M)}{P(b, M)}, \tag{13}$$

where C_{L} and P can be computed according to (11) and (12), respectively. It can be verified that η has the unit of bit / Joule.

In (13), we have explicitly given the dependency of EE on the three design parameters: the spacing between adjacent antennas d, the ADC resolution b, and the number of antennas M. Let the optimal parameters leading to the best EE be denoted with d^*, b^*, and M^*. The maximization of EE is a non-convex problem obviously, since two of the optimization variables, b and M, are integer-valued. Besides, concavity of the capacity lower bound C_{L} in d can neither be obtained due to the oscillation pattern introduced by the sinc function resided in the coupling matrix $\boldsymbol{C}$. As a result, we propose to solve the EE maximization problem by discretizing the domain of d, and applying exhaustive search algorithms. Notice that the power consumption P does not depend on the antenna spacing d, which suggests that d^* is the capacity-maximizing antenna spacing and can be obtained as a function of b and M, by using one-dimensional search. The joint optimization of b and M is also not extremely complex, as b is constrained to a very limited set, and the search for M^* can be accelerated by effective section techniques if necessary.

IV. Numerical Results and Analysis

We perform numerical simulations to learn the optimal antenna array and ADC configuration given different system parameters, and present a number of results in this section. To evaluate the capacity lower bound C_{L}, Monte Carlo simulations are exploited and the results we show in the following are averaged over 2×10^5 independent channel realizations.

A. Capacity-maximizing antenna spacing

As discussed before, the optimal antenna spacing d^* maximizes the lower bound on the ergodic capacity for given M and b. For the unquantized case, we have learned that $d^* < \lambda/2$ for $\theta_0 = 0$, and $\lambda/2 < d^* < \lambda$ for $\theta_0 = \pi/2$. Moreover, for $\theta_0 = 0$, the optimal spacing increases with M and approaches eventually $\lambda/2$ [8]. With Figures 4 and 5 we illustrate the situation with quantized receive signal, where in the search of d^*, the stepsize of 0.005λ has been used. The variation of the capacity lower bound in d is shown in Figure 4 for the end-fire and front-fire directions, respectively. We see that although having only coarsely quantized signals leads to significant loss in capacity, the shape of the curves and the positions of the peaks and valleys remain very much the same. With different numbers of antennas and bit resolutions, we have observed that the optimal antenna spacing is *almost* independent of the ADC resolution employed. When comparing the results of using 1-bit ADC and infinite resolution, some difference in d^* can be found, which is yet small enough to be neglected. In addition, notice that the capacity lower bound in the case of $b = 4$ is nearly as good as the true capacity when having no quantization, which suggests the unnecessariness of using very high bit resolution for the ADC, and also verifies to some extent the effectiveness of employing the capacity lower bound.

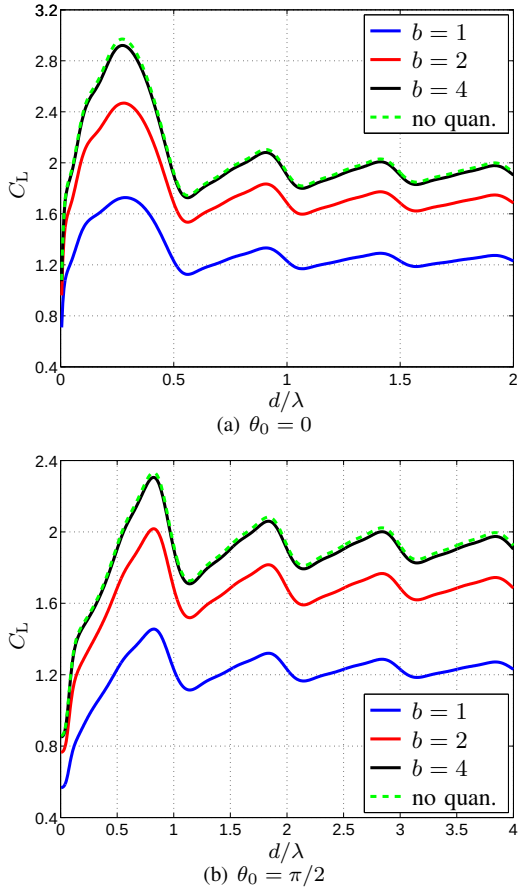

(a) $\theta_0 = 0$

(b) $\theta_0 = \pi/2$

Figure 4. Lower bound on ergodic capacity C_{L} in bit/sec/Hz as dependent on the antenna spacing d ($M = 4$, $\gamma = 0$ dB, $\kappa = 0.01$, $\Delta\theta \to 0$)

Similar to the case without quantization, the optimal antenna spacing is much influenced by the antenna loss factor κ but very insensitive to the average receive SNR γ, as indicated by Figure 5(a). Notice that in the case of $\theta_0 = 0$, although d^* approaches $\lambda/2$ with increasing M, the difference in capacity of employing optimized array and half-wavelength array does not change drastically with M. This can be observed from Figure 5(b), which emphasizes the necessity of optimizing the spacing for a compact ULA of all sizes.

B. Energy efficiency maximizing configuration

For a given bit resolution, since the capacity lower bound increases with reducing rate in M whereas the power consumption grows linearly in M, it can be expected that η as a function of M first increases and then decreases. The value of M at the peak position decreases with improving receive SNR as shown by Figure 6, *i.e.*, with good channel conditions, less antennas are required for achieving the best energy efficiency, while with poor channel conditions, more antennas can be deployed. The bit resolution of the ADC also plays an important role here, making a joint optimization of M and b requisite.

With optimized d and M, the choice for the bit resolution that maximizes the EE depends on the average receive SNR: in general, higher bit resolution can be afforded with good channel conditions, while coarse quantization is more favorable with poor channels. The optimized multi-antenna receiver

ISBN 978-3-8007-3662-1

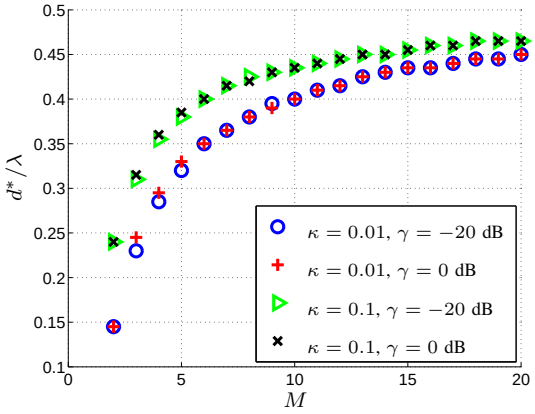

(a) Capacity-maximizing antenna spacing

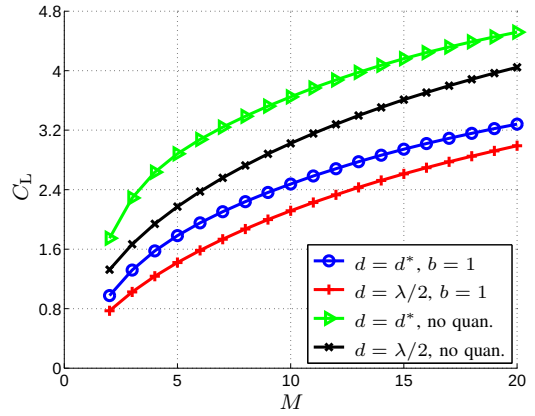

(b) Optimized vs. $\lambda/2$-ULA, $\kappa = 0.01$, $\gamma = 0$ dB

Figure 5. Optimal antenna spacing d^* and lower bound on ergodic capacity C_{L} as dependent on the number of antennas M ($\theta_0 = 0$, $\Delta\theta = \pi/6$)

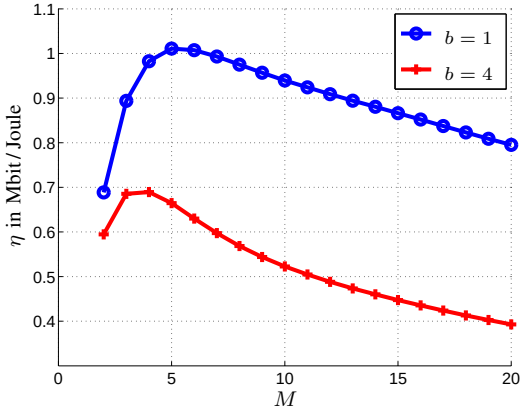

(a) Energy efficiency as dependent on M, $\gamma = -10$ dB

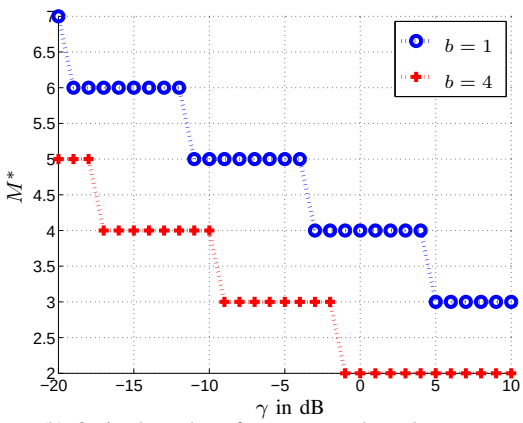

(b) Optimal number of antennas as dependent on γ

Figure 6. Optimizing the number of antennas with fixed bit resolution ($\theta_0 = 0$, $\Delta\theta = \pi/6$, $\kappa = 0.01$, $c_1 = 0.01$)

employs a small number of antennas and low ADC resolution for the set of parameters we have chosen, as shown in Figure 7, which demonstrates the advantage of using small compact antenna arrays when EE is the main performance consideration while low-cost ADC can be employed at the same time. Although the optimization results can be different if other values for the system parameters are taken, the tendency shown here is representative for the communication scenario under investigation.

V. Conclusion

How to optimally configure the compact antenna array and the subsequent A/D conversion to achieve the maximal energy efficiency is the pivot of discussion in this paper. We have focused on a SIMO receiver with a uniform linear array of isotrops, and employed the multiport model to analytically address the impact of antenna mutual coupling. The maximization of energy efficiency, approximated by the ratio between a lower bound on the ergodic capacity of the quantized channel and the power consumption of the receiver, is formulated with respect to the optimization of antenna spacing, the number of antennas, and the ADC resolution. Results from numerical simulations provide the following conclusions:

- The capacity-maximizing antenna spacing depends mainly on the antenna loss factor and the mean angle of arrival, and is almost independent of the bit resolution employed as well as the average receive SNR. Optimized compact array significantly outperforms the half-wavelength spaced array;
- To achieve better energy efficiency, less antennas should be deployed and relatively higher bit resolution should be used if the channel condition is good on average. Otherwise, more antennas are needed while the system should operate with rather low bit resolutions;
- Using compact antenna arrays with a small number of antennas and low precision A/D conversion are two helpful ways to improve the energy efficiency of a multi-antenna receiver, and they can be effectively exploited at the same time.

References

[1] E. Telatar, *Capacity of multiantenna Gaussian channels*, European Trans. on Telecommunications, vol. 10, no. 6, pp. 585-595, November 1999.

[2] G. J. Foschini and M. J. Gans, *On limits of wireless communications in a fading environment when using multiple antennas*, Wireless Personal Communications, vol. 6, no. 3, pp. 311-335, March 1998.

[3] D. Shiu, G. J. Foschini, M. J. Gans and J. M. Kahn, *Fading correlation and its effect on the capacity of multielement antenna systems*, IEEE Trans. on Communications, vol. 48, pp. 502-513, March 2000.

[4] M. Stoytchev, H. Safar, A. L. Moustakas and S. Simon, *Compact antenna arrays for MIMO applications*, in Proc. IEEE Antennas and Propagation Society International Symposium, vol. 3, pp. 708-711, July 2001.

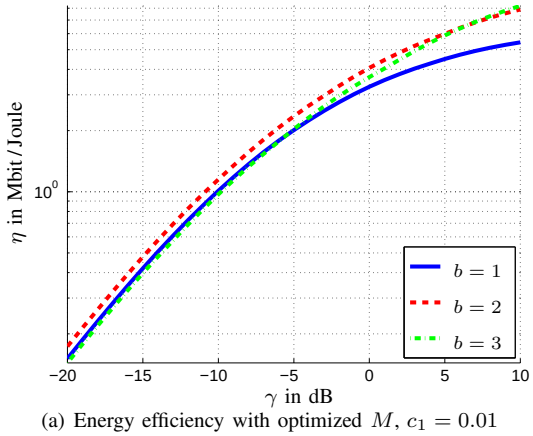

(a) Energy efficiency with optimized M, $c_1 = 0.01$

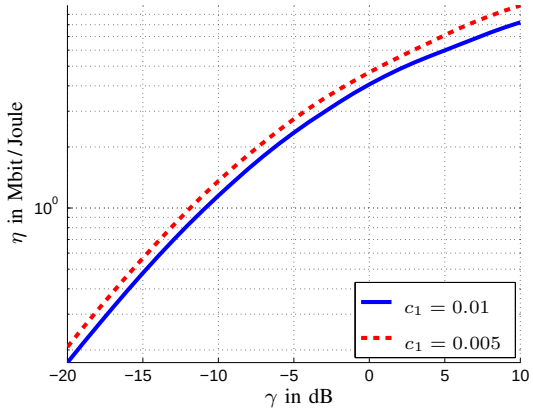

(b) Maximal energy efficiency as dependent on γ

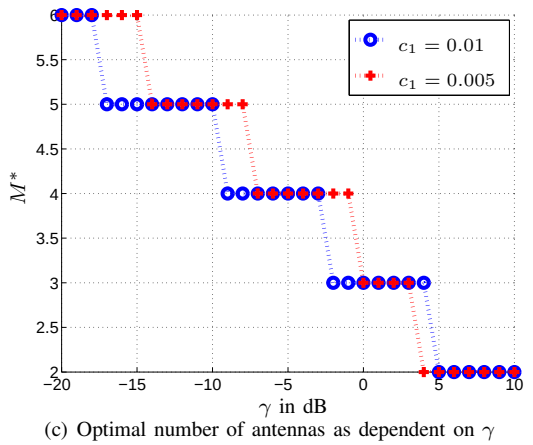

(c) Optimal number of antennas as dependent on γ

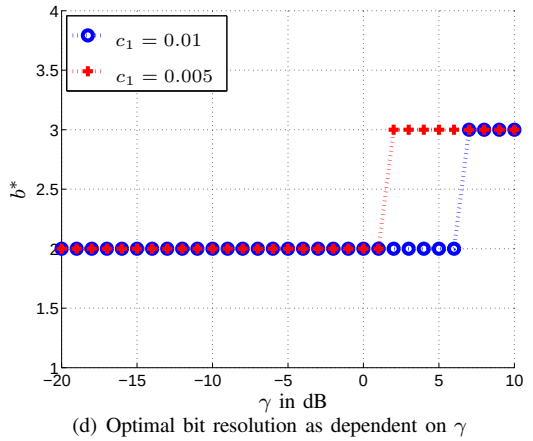

(d) Optimal bit resolution as dependent on γ

Figure 7. Energy efficiency maximization with different γ and c_1 ($\theta_0 = 0$, $\Delta\theta = \pi/6$, $\kappa = 0.01$)

[5] T. Svantesson and A. Ranheim, *Mutual coupling effects on the capacity of multielement antenna systems*, in Proc. 2001 IEEE International Conference on Acoustics, Speech, and Signal Processing, vol. 4, pp. 2485-2488, May 2001.

[6] J. W. Wallace and M. A. Jensen, *Mutual coupling in MIMO wireless systems: a rigorous network theory analysis*, IEEE Trans. on Wireless Communications, vol. 3, pp. 1317-1325, July 2004.

[7] M. T. Ivrlač and J. A. Nossek, *Toward a Circuit Theory of Communication*, IEEE Trans. on Circuits and Systems, vol. 57, no. 7, July 2010.

[8] Q. Bai, A. Mezghani, M. T. Ivrlač and J. A. Nossek, *Optimizing the energy efficiency of SIMO receivers with compact uniform linear arrays*, in Proc. 11th International Symposium on Wireless Communication Systems, August 2014.

[9] B. Murmann, *A/D converter trends: power dissipation, scaling and digitally assisted architectures*, in Proc. IEEE Custom Integrated Circuits Conference, pp. 105-112, September 2008.

[10] J. Singh, O. Dabeer and U. Madhow, *On the limits of communication with low-precision analog-to-digital conversion at the receiver*, IEEE Trans. on Communications, vol. 57, no. 12, pp. 3629-3639, 2009.

[11] A. Mezghani and J. A. Nossek, *Capacity lower bound of MIMO channels with output quantization and correlated noise*, in Proc. IEEE International Symposium on Information Theory, Cambridge, MA, USA, July 2012.

[12] H. S. Lee and C. G. Sodini, *Analog-to-Digital Converters: Digitizing the Analog World*, Proceedings of the IEEE, vol. 96, no. 2, February 2008.

[13] J. J. Bussgang, *Crosscorrelation functions of amplitude-distorted Gaussian signals*, Technical report no. 216, MIT, Cambridge, MA, March 1952.

[14] J. Max, *Quantizing for minimum distortion*, IEEE Trans. on Information Theory, vol. 6, no. 1, pp. 7-12, March 1960.

[15] Q. Bai, A. Mezghani and J. A. Nossek, *On the optimization of ADC resolution in multi-antenna systems*, in Proc. 10th International Symposium on Wireless Communication Systems, August 2013.

[16] S. Cui, A. J. Goldsmith, *Energy-constrained modulation optimization*, IEEE Transactions on Wireless Communications, Sept. 2005, vol. 4, issue 5, pp. 2349-2360.

[17] G. Auer *et al.*, *D2.3: energy efficiency analysis of the reference systems, areas of improvements and target breakdown*, INFSO-ICT-247733 EARTH, ver. 2.0, 2012.

[18] E. Björnson, L. Sanguinetti, J. Hoydis and M. Debbah, *Designing multi-user MIMO for energy efficiency: when is massive MIMO the answer?*, in Proc. IEEE Wireless Communications and Networking Conference, April 2014.

ISBN 978-3-8007-3662-1